K-Dependent Predissociation Dynamics of CS_2 in the 210−216 nm Region

Jun Chen, Ying Guo, Xiaoguo Zhou, Yong Shi, Shilin Liu,* and Xingxiao Ma

Hefei National Laboratory for Physical Sciences at Microscale, Department of Chemical Physics, University of Science and Technology of China, Hefei, Anhui 230026, China

Received: September 21, 2006; In Final Form: April 24, 2007

The dependence of CS_2 predissociation upon rotational quantum number *K* at vibrational levels below the barrier to linearity of the $^1B_2(^1\Sigma_u^+)$ state has been investigated in detail with laser spectroscopy, by using a heated supersonic source to increase the intensities of hot band transitions. Predissociation lifetimes were determined from rotational contour simulations of 13 vibronic bands in the CS photofragment excitation (PHOFEX) spectrum, each terminating at the same upper vibrational level but via transitions with different *K* number ($K = 0$, 1, 2, respectively). The rovibrational populations of CS fragment at these excitation bands were derived from the laser-induced fluorescence (LIF) spectrum, and were used further to obtain the dissociation branching ratios $S(^1D)/S(^3P)$ as well as the excess energy partitionings after dissociation. The lifetimes and the branching ratios were found to be sensitively dependent on quantum number K; the lifetime decreases with the increase of *K*, and the branching ratio increases with *K*. Analysis shows that quantum number *K* influences the $S(^1D)$ channel more effectively than the $S(^3P)$ channel. About 28 and 15% of the total available energy is taken up by the CS vibrational and rotational degrees of freedom, respectively. Systematic analysis indicates that the two electronic states interacting with $^1B_2(^1\Sigma_u^+)$ state should be bent, and the state correlating with $S(^1D)$ channel should be more bent.

1. Introduction

The strongest absorption band of CS_2 molecule in the wavelength range of 185−230 nm, which was assigned as $^1B_2(^1\Sigma_u^+) \leftarrow X^1\Sigma_g^+$ parallel electronic transition, has been investigated by numerous authors.[1−8] The band origin, equilibrium bond length and angle, and the vibrational frequencies of the $^1B_2(^1\Sigma_u^+)$ state were determined from the spectrum in this range. The spectroscopic analyses indicate that there is an energetic barrier in the $^1B_2(^1\Sigma_u^+)$ state located at around 204 nm for molecular structure changing from bent to linear geometry.[2,7,8] Extensive studies have been performed on the dissociation dynamics of CS_2 in the $^1B_2(^1\Sigma_u^+)$ state.[9−23] It has been known that CS_2 molecule in this excited state is predissociative via two parallel pathways, $CS_2(^1B_2(^1\Sigma_u^+)) \rightarrow CS(X^1\Sigma^+) + S(^3P)$ and $CS_2(^1B_2(^1\Sigma_u^+)) \rightarrow CS(X^1\Sigma^+) + S(^1D)$. Detailed information about dissociation dynamics such as the lifetimes,[5,6,15,17−22] the branching ratio $S(^3P)/S(^1D)$,[9−15,23] and the excess energy partitioning,[9,10,13,16,17] had been obtained.

Most of the photodissociation studies of CS_2 molecule were carried out at excitation wavelengths around 200 nm. In this energy region, CS_2 molecule can be excited to energy levels above the geometric conversion barrier of the $^1B_2(^1\Sigma_u^+)$ state, that is, the molecule will dissociate in linear configuration. The lifetime was estimated to be in a range of 1−2 ps, the branching ratio $S(^3P)/S(^1D)$ was measured to be around 2.8, and more than half of the excess energy was partitioned into the CS internal degrees of freedom, especially the vibrational motion.[9,10,13,22] But what happens for CS_2 molecule below the barrier of the $^1B_2(^1\Sigma_u^+)$ state, that is, CS_2 molecule in bent configuration, still remains unclear. The detailed studies had been carried out by Hepburn and his co-workers.[5, 13−15] In their studies, the predissociation lifetimes and the branching ratio $S(^3P)/S(^1D)$ in the wavelength range of 198 - 220 nm, were derived from the (1 + 1) resonance-enhanced multiphoton ionization (REMPI) spectrum and the detection of $S(^3P)$ and $S(^1D)$ fragments by vacuum ultraviolet (VUV) laser-induced fluorescence (LIF). They found a trend that the predissociation dynamics of CS_2 in the $^1B_2(^1\Sigma_u^+)$ excited state is affected by the initial transition states, especially the bending vibration (quantum number $v_{2''}$) and/or the vibrational angular momentum (quantum number l''). For a vibrational level of the $^1B_2(^1\Sigma_u^+)$ state, the lifetime of CS_2 via $(K = 1) \leftarrow (v_{2''} = 1, l'' = 1)$ excitation is shorter than that via $(K = 0) \leftarrow (v_{2''} = 0, l'' = 0)$ excitation. Here, *K* is the rotational quantum number of CS_2 in $^1B_2(^1\Sigma_u^+)$ state. Furthermore, CS_2 molecule via $(K = 1) \leftarrow (v_{2''} = 1, l'' = 1)$ excitation has a higher yield of $S(^1D)$ product than that via $(K = 0) \leftarrow (v_{2''} = 0, l'' = 0)$ excitation. They concluded that the predissociation process depends on the number *K*.

In order to conclusively relate predissociation lifetimes to the *K* values of transitions and examine its extension validity to higher *K*, and to explore the influence of *K* on the branching ratio, the rovibrational populations of CS fragment as well as the excess energy partitioning among various degrees of freedom, a heated supersonic source (∼130 °C) was used in present work to increase the fraction of vibrationally excited molecules in the beam and hence the transition intensities of hot bands, allowing us to reach higher *K* sublevels within each vibrational level of the $^1B_2$ state. The CS_2 lifetimes were determined from the rotational contour simulations of totally 13 vibronic bands via excitations of different *K* numbers in the CS PHOFEX spectrum. The rovibrational populations of CS fragment from these excitation bands, which remain unknown from literatures, were derived from the LIF spectrum. The populations were decomposed into two parts corresponding to the contributions from two dissociation channels, $CS(X^1\Sigma^+)$ +

* Author to whom correspondence should be addressed. E-mail: slliu@ustc.edu.cn.

10.1021/jp0661894 CCC: $37.00
Published on Web 06/05/2007

$S(^3P)$ and $CS(X^1\Sigma^+) + S(^1D)$, and were then employed to obtain the branching ratio and the released energy partitionings into rotational, vibrational and translational degrees of freedom of the CS fragment. These data provide some further insight into the fragmentation dynamics of CS_2 at vibrational levels below the barrier to linearity in the $^1B_2(^1\Sigma_u^+)$ state.

2. Experimental Section

The setup for present experiment consists of three parts, (i) a heated pulsed supersonic beam source to rotationally cool CS_2 molecules and remain vibrationally hot, (ii) an Nd:YAG pumped two tunable dye lasers, and (iii) LIF signal detection and data acquisition system. The timing sequence among the pulsed valve, the lasers, and the data collection hardware was controlled by a pulse generator (Stanford, DG535).

The jet-cooled CS_2 molecules were produced from supersonic expansion of CS_2/He (1%) gas mixture through a pulsed valve (General Valve series 9, nozzle diameter 0.5 mm) into a vacuum chamber. To increase the population of vibrationally excited CS_2 molecules, the gas mixture was preheated to 50 °C prior to expansion, and then passed the valve which was heated to 130 °C. It was estimated that at temperature of 130 °C the relative populations of (0, 3, 0) overtone level is increased by 3 times higher than that at room temperature, ~3% of total number density of CS_2 molecules. The vacuum chamber was pumped by two turbo-molecular pumps (1500 *l*/s), which were backed up by two mechanical pumps (15 *l*/s). The stagnation pressure was kept at ~1atm, and the operating pressure in the chamber was about 1×10^{-6} Torr.

Two dye lasers (Sirah, PRSC-LG-18 and PRSC-LG-24, line width 0.07 cm^{-1}), pumped simultaneously by the third harmonic output of an Nd:YAG laser (Spectra Physics, Lab-190), were employed in this experiment. The frequency doubled output of one dye laser, in the wavelength range of 209.5−216 nm with intensity of 50−80 μJ/pulse, was used as the excitation/dissociation light to excite CS_2 molecule from its ground state $X^1\Sigma_g^+$ to electronically excited state $^1B_2(^1\Sigma_u^+)$. The frequency-doubled output of another dye laser, 20−50 μJ/pulse, was used to record the LIF spectrum of CS fragment in the range of 247−287.5 nm. The two laser beams counter-propagated and spatially overlapped with each other, and crossed the molecular beam perpendicularly at a distance of 20 mm downstream from the nozzle orifice. The probe laser was optically delayed by 10ns relative to the excitation laser. When the CS photofragment excitation (PHOFEX) spectrum was measured, the wavelength of excitation laser was scanned, and the probe laser was fixed at 257.6 nm, corresponding to the head position of Q-branch of CS $A^1\Pi(v' = 0) \leftarrow X^1\Sigma^+(v'' = 0)$ transition. When the LIF spectrum of CS fragment was recorded, the probe laser was scanned and the excitation laser was fixed respectively at wavelengths corresponding to vibronic transitions of CS_2 molecule, that is, 210.27 nm (Σ_0^g), 213.85 nm (Σ_2^g), 211.95 nm (Π_1^g), and 213.57 nm (Δ_2^g). In order to avoid saturation effect during the experiment, two optical telescopes with two pairs of convex lenses were used to expand both laser beams and hence to reduce the photon densities in the laser-molecule interaction region. Otherwise, saturation would occur as confirmed by our power dependence measurement, although pulse intensities of the two lasers are quite low.

The laser-induced fluorescence of CS fragment was collected with a couple of lenses and detected with a photomultiplier tube (Hamamasu, R2460). The LIF signal was amplified with a preamplifier (Stanford, SR240), averaged by a boxcar averagers (Stanford, SR250), and then interfaced to a PC for data storage.

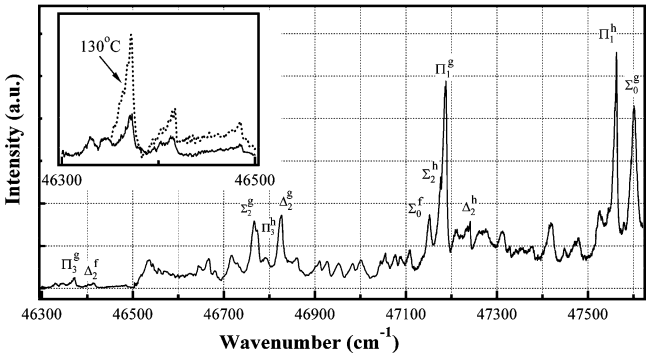

Figure 1. PHOFEX spectrum of CS_2 in the wavelength range of 210−216 nm by monitoring the fluorescence of CS fragment from the excitation of Q-branch of $A^1\Pi(v' = 0) \leftarrow X^1\Sigma^+(v'' = 0)$ transition at 257.6 nm. The spectrum was recorded at room-temperature stagnation conditions. The insertion in figure is a comparison of spectrum recorded under normal conditions (solid line) with that by heating the supersonic nozzle to 130 °C (dashed line). Significant increase of hot band transitions can been seen.

During the experiment, the wavelengths of two lasers were calibrated simultaneously against the argon optogalvanic spectrum resulting in an overall absolute uncertainty of 0.5 cm^{-1} in the excitation energy, and the intensities of both lasers were monitored simultaneously with two photodiodes to normalize the spectra.

3. Results and Discussion

3.1. *K*-Dependent Predissociation Lifetimes of CS_2. The PHOFEX spectrum of CS_2 was obtained by fixing the wavelength of probe laser at 257.6 nm and scanning the wavelength of dissociation laser in the range of 209.5−216 nm, as shown in Figure 1. The spectral assignment was adopted from previous works by Douglas and Zanon[1] and Beatty et al.[5] Due to the near degeneracy of ν_1 and ν_2 vibrational modes at the $^1B_2(^1\Sigma_u^+)$ state, the vibrational levels could not be presented by normal mode (ν_1, ν_2, ν_3),[1] and were just marked as a, b, c..., in the order of increasing energy. Since spectral analysis showed that CS_2 molecule at the $^1B_2(^1\Sigma_u^+)$ state was a near-prolate symmetric top,[1] the electronic transition $^1B_2(^1\Sigma_u^+) \leftarrow X(^1\Sigma_g^+)$ of this spectrum is parallel. Due to selection rules for a parallel transition, the rotational quantum number K in the upper vibrational levels always correlates with the vibrational angular momentum l'' in the lower vibrational levels, $K \equiv l''$. Vibronic transitions between $^1B_2(^1\Sigma_u^+)$ and $X(^1\Sigma_g^+)$ electronic states are labeled as Σ, Π, Δ..., corresponding to K ($=l''$) = 0, 1, 2..., subscripts are used to denote the bending vibrational quantum number in the ground state, $\upsilon_{2''}$, and the superscripts indicate the upper vibrational levels (a, b, c...).

Based on the spectral constants of CS_2 at the $^1B_2(^1\Sigma_u^+)$ state in literatures,[1,2] vibronic transitions to the f, g and h vibrational levels were identified in Figure 1. As seen from the insertion in Figure 1, the weak hot bands, Δ_2^f and Π_3^g under stagnation conditions of room temperature, became significantly stronger when the sample gas was heated to 130 °C. The hot band intensities was increased by 2~3 times, which enabled us to record the hot band transitions with sufficient variations of K number, and in turn to investigate the influence of K ($=l''$) on the predissociation of CS_2 in a broader range.

Predissociation lifetimes of CS_2 at the f, g, and h vibrational levels of the $^1B_2(^1\Sigma_u^+)$ state were obtained from simulations of the rotational contours in the PHOFEX spectrum with parameter of dissociation-broadened line width (lifetime), as described in the refs 15 and 17. During the spectral simulation, an assumption

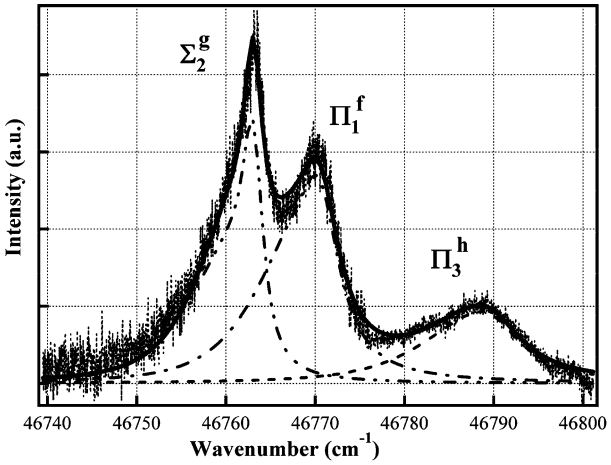

Figure 2. Simulation of three overlapping rotational contours in the PHOFEX spectrum of CS_2. Solid line represents the overall fitting to the three contours. Rotational temperature to best fit the whole spectrum was 30 K. Dissociation lifetimes of the g, f, and h states were determined from the spectral fitting.

was made that the lifetimes of rotational levels within a vibrational state were identical for all J'. Since the rotational temperature of CS_2 in our experiment was about 25 K, as estimated from the LIF spectrum of NO under similar jet expansion conditions, only low J'' rotational levels could be excited. Stimulated emission pumping experiment by Liou et al.[24] shows that the lifetimes of rotational levels ranging from $J' = 5$ to 17 are insensitive to J', indicating our assumption is reliable.

Figure 2 shows an example of our spectral fittings to the three congested rotational contours. A complete reporting of all our results will appear in detail in a future paper. The determined lifetimes of our interested vibrational levels via excitations of different quantum number *K* are listed in Table 1. The lifetimes reported in refs 5, 15, and 17 are also listed in this table for comparison. Generally, the majority of the predissociation lifetimes from this work agree within experimental error with those previously reported. The lifetimes in refs 5 and 15 were reported by Hepburn's group with different spectroscopic method. Results in ref 15 were deduced from the band contour simulations by detecting S-atom products with vacuum ultraviolet laser-induced fluorescence (VUV-LIF), and the data in ref 5 were derived from the (1 + 1) REMPI spectrum. Slight differences exist between these two sets of data measured by the same group. Compared to the data in ref 5, our results are closer to the data in ref 15 obtained from the VUV-LIF spectrum. As already stated in section 2, saturation effect should be avoided even though the laser intensity is quite low. In fact, changes of band shape with different focusing conditions had been noticed in ref 5, implying that saturation effect or power broadening might exist in the (1 + 1) REMPI spectrum.[5] The determined lifetime for Σ_0^g band in ref 17 is slightly longer than all of the available results for unknown reasons.

It can be seen from Table 1 that for the same upper vibrational level the predissociation lifetime is quite different for different transition. It is clear that the difference of lifetime is not caused by the energy difference in upper state, since the energy difference for $K = 0$, 1, and 2 sublevels in the same vibrational state is small (57 cm^{-1} maximum).[5] The lifetime difference must arise from the change of initial transition state, $l''(=K)$ or/and $v_{2''}$. In order to clarify the influences of *K* and $v_{2''}$ on lifetime, several pairs of transitions with the same *K* but different $v_{2''}$ were compared, such as Σ_0^g and Σ_2^g, Σ_2^h and Σ_4^h, Π_1^g and Π_3^g, and Π_1^h and Π_3^h, it is evident from Table 1 that the bending quantum number $v_{2''}$ has little effect on predissociation lifetime, since the lifetime does not change obviously for different $v_{2''}$. Contrarily, comparison of transitions with the same $v_{2''}$ but different *K*, such as Σ_2^g and Δ_2^g, Σ_2^h, and Δ_2^h, shows that *K* has a distinct influence on lifetime. We obtained lifetimes for the f, g, and h vibrational states, and for each states transitions with quantum numbers $K = 0$, 1, and 2 were measured. Therefore, it becomes certain that within a vibrational state the lifetime of CS_2 is governed by quantum number *K*; the lifetime decreases with the increase of *K*, which applies at least to $K = 0$, 1, and 2 regardless of the vibrational states.

3.2. Rovibrational Populations of CS Fragment and the Branching Ratios. Measurement of internal state distributions of CS fragment can provide further insight into the dissociation procedure of CS_2 molecules at the $^1B_2(^1\Sigma_u^+)$ state. As far as we know from literatures, all studies about rovibrational population of CS fragment have focused on the dissociation at 193 nm,[9,16,22] there has been no report at dissociation wavelengths below the barrier to linearity of $^1B_2(^1\Sigma_u^+)$ state until now. In order to measure the internal state distributions of CS and to examine the influences of quantum number *K*, LIF spectra of CS fragment were recorded for the g vibrational state through excitations, Σ_0^g, Σ_2^g, Π_1^g, and Δ_2^g, respectively. Figure 3 shows the LIF spectrum of nascent CS fragment for CS_2 photodissociation at 211.95 nm (Π_1^g band). The spectrum originates from ($A^1\Pi$, v') ← ($X^1\Sigma^+$, v'') vibronic transition of CS in the wavelength range of 287.5−247 nm, and is assigned in terms of (v', v'').[22, 25] Sharp peaks in the spectrum are rotational

TABLE 1: The Determined Lifetimes of CS_2 from Rotational Contour Simulations at the f, g, and h Vibrational Levels of $^1B_2(^1\Sigma_u^+)$ State via Excitations of Different Quantum Number *K*

vibrational state	assignment	position (cm^{-1})	lifetime (ps) this work	ref 15	ref 5	ref 17
f	Σ_0^f	47147.4	1.3 ± 0.2	1.6 ± 0.3	1.6 ± 0.2	
	Π_1^f	46770.0	1.0 ± 0.2	1.2 ± 0.5	1.1 ± 0.2	
	Δ_2^f	46417.2	0.8 ± 0.1			
g	Σ_0^g	47557.1	2.1 ± 0.2	2.8 ± 0.3	3.3 ± 0.8	4.4
	Σ_2^g	46762.0	2.2 ± 0.2		2.0 ± 0.3	
	Π_1^g	47181.3	1.8 ± 0.2	1.2 ± 0.3	1.9 ± 0.2	
	Π_3^g	46374.5	1.6 ± 0.2			
	Δ_2^g	46822.0	1.2 ± 0.2	1.3 ± 0.3	0.5 ± 0.2	
h	Σ_2^h	47169.2	1.8 ± 0.4			
	Σ_4^h	46363.0	1.7 ± 0.4			
	Π_1^h	47596.1	0.5 ± 0.2	0.55 ± 0.15		
	Π_3^h	46788.9	0.6 ± 0.2			
	Δ_2^h	47230.3	0.5 ± 0.1		1.0 ± 0.2	

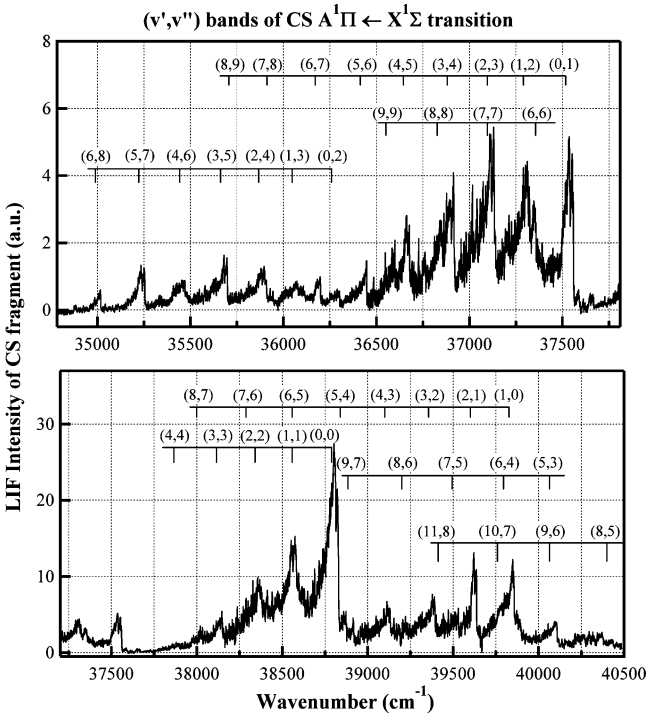

Figure 3. LIF spectrum of nascent CS fragment from photodissociation of CS_2 at 211.95 nm (Π_1^g band) through ($A^1\Pi$, v') ← ($X^1\Sigma^+$, v'') vibronic transitions in the wavelength range of 287.5−247 nm. The spectrum is assigned in terms of (v', v'').

structures of CS, rather than the experimental noise. An expansion view of the (4, 6) band is shown in Figure 4, and can be assigned unambiguously. As can be seen, rotational lines are resolved completely, enabling us to derive the relative rotational population $P_{v'',J''}$ of CS($X^1\Sigma^+$, v'') fragment.

From the rotationally resolved LIF spectra of CS($X^1\Sigma^+$) fragment, the relative rotational populations $P_{v'',J''}$ at J'' rotational level of the v'' vibrational state could be derived with their rotational line intensities, Hönl-London factors $S_{J',J''}$, and Franck−Condon factors $f_{v',v''}$:

$$P_{v'',J''} = I_{v',J'\leftarrow v'',J''}/S_{J',J''}f_{v',v''} \quad (1)$$

and the relative vibrational populations $P_{v''}$:

$$P_{v''} = \sum_{J''} P_{v'',J''} \quad (2)$$

could be obtained straightly. We recorded the rotational structures of (0,0), (0,1), (0,2), (1,3), (2,4), (3,5), (4,6), (5,7), and (6,8) vibrational bands in CS ($A^1\Pi$) ← ($X^1\Sigma^+$) transition, which overlap with each other not seriously as shown in Figure 3. With the aids of spectral constants and transition factors given by Bergeman and Cossart,[25] the relative rotational and vibrational populations of CS fragment for $v'' = 0-8$ were obtained following eqs 1 and 2.

Figure 5 shows the relative vibrational populations of nascent CS($X^1\Sigma^+$,v'') from CS_2 photodissociation through the Σ_0^g, Σ_2^g, Π_1^g and Δ_2^g excitations. As can be seen, the vibrational distribution of CS fragment does not follow a thermodynamic equilibrium distribution. Comparing to the results at 193 nm,[16] where vibrational levels up to $v'' = 12$ were found to be populated in a bimodal distribution peaking at $v'' = 4$ and 8, the difference between our results and those at 193 nm indicates that the dissociation dynamics below and above the barrier to linearity should be quite different. Since in the present excitation energy range, two parallel dissociation channels exist:

$$CS_2(X^1\Sigma_g^+) + h\nu \rightarrow CS_2(^1B_2(^1\Sigma_u^+)) \rightarrow CS(X^1\Sigma^+) + S(^3P)$$
$$D_0 = 4.46 \text{ eV } (35970 \text{ cm}^{-1}) \quad (3)$$

$$\rightarrow CS_2(X^1\Sigma^+) + S(^1D)$$
$$D_0 = 5.61 \text{ eV } (45200 \text{ cm}^{-1}) \quad (4)$$

where D_0 is the dissociation energy for the corresponding channel.[26] Therefore, our measured vibrational distribution of CS consists of contributions from the two dissociation channels. Since the vibrational frequency of CS($X^1\Sigma^+$) is 1285.15 cm^{-1},[25] the populated vibrational state of CS($X^1\Sigma^+$) from the S(^{1}D) channel cannot exceed $v'' = 1$ in present study. Consequently, the measured vibrational distribution of CS can be divided into two regions; populations at $v'' = 2-8$ come from the S(^{3}P) channel, and populations at $v'' = 0$ and 1 include contributions of both channels. Furthermore, Lee and Judge[27] reported that the vibrational population of CS($X^1\Sigma^+$, v'') fragment could be represented by a Poisson distribution as derived from an impulsive half-collision model:

$$P_{v''} = N_1(\Delta E)^{v''-1}\frac{(\Delta E)^2 + (\alpha - 2v'')\Delta E + v''^2}{v''![(\Delta E)^2 + (\alpha - 2)\Delta E + 1]} \quad (5)$$

where N_1 is an intensity factor, ΔE and α are the parameters. With this expression, the vibrational distribution of CS from S(^{3}P) channel was simulated first for $v'' = 2-8$, and then extended to the entire range as shown in Figure 5. The vibrational distribution associated with the S(^{1}D) channel at $v'' = 0$ and 1 was obtained by subtracting the contribution of S(^{3}P) channel from the measured total vibrational distribution, as also shown in Figure 5. In this way, the relative vibrational populations of CS fragment from the two dissociation channels were obtained. Consequently, the branching ratio Φ = S(^{3}P)/S(^{1}D) could be determined:

$$\Phi = \sum_{v''=0}^{8} P_{v''}[S(^3P)]/\sum_{v''=0}^{1} P_{v''}[S(^1D)] \quad (6)$$

The determined branching ratios for CS_2 dissociated through the Σ_0^g, Σ_2^g, Π_1^g, and Δ_2^g excitations are listed in Table 2.

The branching ratio S(^{3}P)/S(^{1}D) through Σ_0^g excitation is very similar with that throught Σ_2^g excitation, thus the initial bending vibrational quantum number $v_{2''}$ has little effect on S(^{3}P)/S(^{1}D). In contrast, the branching ratios through Δ_2^g and Σ_2^g excitations differ greatly, indicating that the branching ratio is sensitively dependent on K (=l''). The trend of branching ratio with K in Table 2 means that increasing K can promote the dissociation of CS_2 molecules into the CS($X^1\Sigma^+$) + S(^{1}D) channel. This conclusion is similar to those in section 3.1 that the predissociation lifetime is governed by K not $v_{2''}$, and decreases with the increase of K.

Combining the lifetimes τ in Table 1 and the branching ratios Φ in Table 2, the dissociation rate of CS_2 for dissociation channels S(^{3}P) and S(^{1}D) could be derived. The dissociation rate of CS_2 can be expressed as

$$r = \frac{1}{\tau} = r(^3P) + r(^1D) \quad (7a)$$

$$\Phi = r(^3P)/r(^1D) \quad (7b)$$

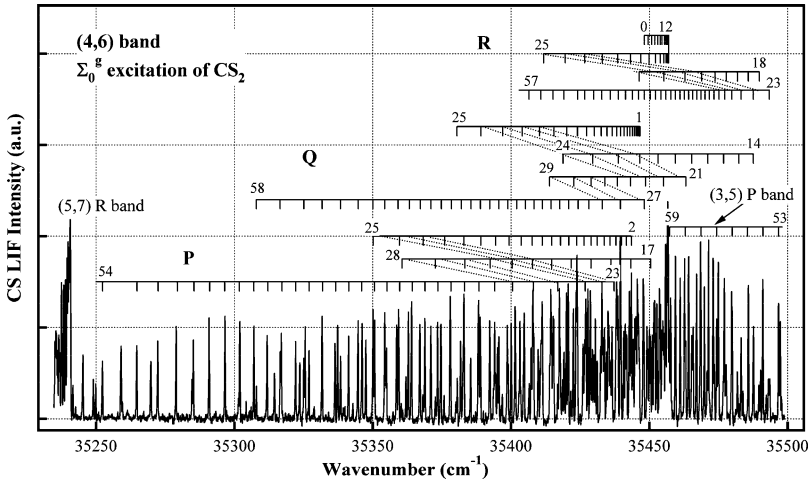

Figure 4. Expansion of the LIF spectrum in Figure 3 in the region of (4, 6) band of CS fragment. Rotational lines are resolved distinctly, making it possible to obtain the relative rotational distribution of $CS(X^1\Sigma^+)$ at $v'' = 6$ vibrational state.

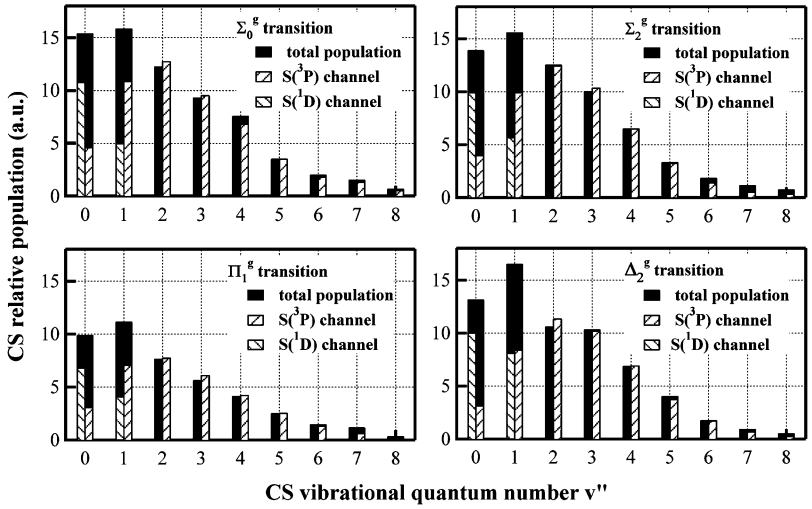

Figure 5. Relative vibrational populations from the rotationally resolved LIF spectra of nascent CS ($X^1\Sigma^+$, v'') for CS_2 photodissociations through the Σ_0^g, Σ_2^g, Π_1^g, and Δ_2^g excitations. The solid bar represents experimental results. The population from $S(^3P)$ channel was simulated following eq 5 in the text, and that from $S(^1D)$ channel was obtained by subtracting the contributions of $S(^3P)$ channel from the measured total vibrational distributions for $v'' = 0$, 1.

TABLE 2: The Dissociation Branching Ratios $S(^3P)/S(^1D)$ and Dissociation Rates of $CS(X^1\Sigma^+) + S(^3P)$ and $CS(X^1\Sigma^+) + S(^1D)$ Channels for the g Vibrational State of CS_2 through Different Excitations

transition	position (cm^{-1})	branching ratio Φ $S(^3P)/S(^1D)$	lifetime τ (ps)	rate $r(^3P)$ (ps^{-1})	rate $r(^1D)$ (ps^{-1})
Σ_0^g	47557.1	5.6 ± 1.2	2.1 ± 0.2	0.40	0.07
Σ_2^g	46762.0	5.5 ± 1.2	2.2 ± 0.2	0.38	0.07
Π_1^g	47181.3	3.4 ± 0.8	1.8 ± 0.2	0.43	0.13
Π_3^g	46374.5		1.6 ± 0.2		
Δ_2^g	46822.0	2.7 ± 0.6	1.2 ± 0.2	0.61	0.23

where $r(^3P)$ and $r(^1D)$ represent the dissociation rate following $S(^3P)$ and $S(^1D)$ channels, respectively. Substituting determined values of τ and Φ into eq 7, the dissociation rates $r(^3P)$ and $r(^1D)$ for the g vibrational level of $^1B_2(^1\Sigma_u^+)$ state were obtained, and also listed in Table 2. We may conclude from Table 2 that both of dissociation rates $r(^3P)$ and (^1D) increase with K, but the increasing magnitude of $r(^1D)$ is larger than that of $r(^3P)$. In other words, the increase of K accelerates the dissociation and tends to proceed along the $CS(X^1\Sigma^+) + S(^1D)$ pathway.

3.3. Partitioning of Total Available Energy after Dissociation. On the basis of the obtained rotational and vibrational populations, $P_{v'',J''}$ and $P_{v''}$, the partitioning of total available energy for the two dissociation channels could be evaluated. The total available energy is define as $E_{avl} = h\nu + E_{int} - D_0$, where E_{int} is the internal energy of CS_2 molecule at the initial transition state, and $h\nu$ is the excitation photon energy. The average rotational energy of CS fragment from the $CS(X^1\Sigma^+) + S(^3P)$ channel is derived from

$$\langle E_{rot} \rangle = \sum_{v''} \sum_{J''} P_{v'',J''} E_{J''} / \sum_{v''} \sum_{J''} P_{v'',J''} \qquad (8)$$

and the average vibrational energy of CS from the $CS(X^1\Sigma^+) + S(^3P)$ channel is from

$$\langle E_{vib} \rangle = \sum_{v''} P_{v''} E_{v''} / \sum_{v''} P_{v''} \qquad (9)$$

where $P_{v'',J''}$ and $P_{v''}$ are defined in eqs 1 and (2), $E_{J''}$ and $E_{v''}$ represent rotational and vibrational energies at J'' and v'' states, respectively. Since the measured populations $P_{v'',J''}$ of $CS(X^1\Sigma^+)$ at $v'' = 0$ and 1 consist of contributions from the two dissociation channels, $P_{v'',J''}$ at $v'' = 0$ and 1 for the $CS(X^1\Sigma^+) + S(^3P)$ channel was obtained by scaling the measured $P_{v'',J''}$ with the ratio of simulated $P_{v''}$ using eq 5 to the measured total $P_{v''}$. In this way, the partition ratios of available energy into the rotational, vibrational and translational degrees of freedom of

TABLE 3: Partitioning of the Total Available Energy for CS_2 Dissociation at the $^1B_2(^1\Sigma_u^+)$ State into $CS(X^1\Sigma^+) + S(^3P)$ and $CS(X^1\Sigma^+) + S(^1D)$ Products

dissociation channel	transition	E_{avl} (cm^{-1})	$\langle E_{vib}\rangle/E_{avl}$	$\langle E_{rot}\rangle/E_{avl}$	$\langle E_{trans}\rangle/E_{avl}$
$CS(X^1\Sigma^+) + S(^3P)$	Σ_0^g	11567	0.26	0.15	0.58
	Σ_2^g	11567	0.25	0.15	0.59
	Π_1^g	11583	0.28	0.16	0.56
	Δ_2^g	11625	0.30	0.15	0.54
$CS(X^1\Sigma^+) + S(^1D)$	Σ_0^g	2332	0.16		
	Σ_2^g	2332	0.17		
	Π_1^g	2348	0.20		
	Δ_2^g	2390	0.25		

the fragments for dissociation along the $S(^3P)$ pathway were obtained, and listed in Table 3. For the $S(^1D)$ channel, we just presented the vibrational energy partition ratios, since the populations for this channel could not be obtained directly from experiment.

Comparing our results carried out below the barrier to linearity with those at dissociation wavelength of 193 nm above the barrier, two distinct differences can be found: (1) in the present study, the partitioning of total available energy into rotational degree of CS fragment from the $S(^3P)$ channel is about 15%, bigger than that of ~7% for photodissociation at 193 nm which was reported by several groups;[9,10,22] (2) the partition into vibrational degree, ~28%, becomes distinctly smaller than ~50% at 193 nm. For the $S(^3P)$ channel, these two points of difference indicate that CS_2 molecules at vibrational levels below the barrier to linearity dissociate with a more bent configuration than that above the barrier. Frey and Felder[28] pointed out that the dissociation at 193 nm through $S(^3P)$ channel seems to occur mainly at the linear configuration. Moreover, as can be seen from Table 3, vibrational energy partition ratios of CS through the $S(^1D)$ channel, ~20%, are smaller than those through the $S(^3P)$ channel, ~28%, suggesting that CS_2 molecule through the $S(^1D)$ channel is more bent than that through the $S(^3P)$ channel. Furthermore, a trend seems to exist in Table 3, that with the increase of quantum number *K* the vibrational energy partition ratios for both channels increase, and similar to the behaviors of dissociation rates for both channels, the increasing magnitude for the $S(^1D)$ channel is larger than that for the $S(^3P)$ channel. More works about other vibrational levels of the $^1B_2(^1\Sigma_u^+)$ state are required in order to conclusively relate the vibrational energy partition ratio to *K* values.

Hepburn et al. [5,15] indicated that the $CS(X^1\Sigma^+) + S(^3P)$ channel is resulted from a spin−orbit coupling between the initially excited $^1B_2$ state and a triplet linear repulsive state ($^3\Pi$ or $^3\Sigma_g$), and the $CS(X^1\Sigma^+) + S(^1D)$ channel occurs through the crossing of the $^1B_2$ state with another singlet linear repulsive state ($^1\Pi$). Base on our experimental results and previous studies,[28] we are inclined to state that at energies below the barrier to linearity, both geometries of the singlet and triplet states through which CS_2 molecule predissociates should be bent, not linear. Moreover, the singlet repulsive state should be more bent than the triplet repulsive state. With this tentative assumption, our experimental findings can be explained reasonably. Since the quantum number *K* describes the rotation along a main axis parallel to the S−S connection line of CS_2 molecule, the centrifugal force will promote the molecular geometry to be more bent. The higher the *K* value is, the more bent the CS_2 molecules become, and the more stronger coupling between the $^1B_2(^1\Sigma_u^+)$ state and a more bent singlet repulsive state, resulting in the acceleration of dissociation along the $S(^1D)$ pathway.

4. Summary

Predissociation dynamics of CS_2 at vibrational energy levels of the $^1B_2$ ($^1\Sigma_u^+$) state below the barrier to linearity has been studied by measuring the lifetimes and the rovibrational population distributions of CS fragment with photofragment excitation (PHOFEX) spectroscopy and laser-induced fluorescence (LIF) spectroscopy. Emphases were paid to the investigation of the relationship between these measurements and the rotational quantum number *K*, by using a heated nozzle to increase the hot band transition and hence the value of *K*. It was found that with the increase of *K* the lifetime decreases greatly, and the branching ratio of two channels $S(^1D)/S(^3P)$ increases. These two kinds of results led to a conclusion that the increase of *K* accelerates dissociation rate for both channels, but influences the $S(^1D)$ channel more effectively. Furthermore, analyses of rovibrational population distributions showed that the molecular configurations along the two dissociation pathways should be bent, and CS_2 molecule along the $S(^1D)$ pathway should be more bent than along the $S(^3P)$ pathway. Possible explanation was presented that the two electronic states through which CS_2 molecule predissociates are bent, and the singlet state to form $S(^1D)$ channel is more bent than the triplet state to form $S(^3P)$ channel.

Acknowledgment. The present work was supported financially by the National Natural Science Foundation of China (NSFC, No. 20533070, No. 20573100, No. 20373066).

References and Notes

(1) Douglas, A. E.; Zanon, I. *Can. J. Phys*. **1964**, *42*, 627.
(2) Hemley, R. J.; Leopold, D. G.; Roebber, J. L.; Vaida, V. *J. Chem. Phys.* **1983**, *79*, 5219.
(3) Roebber, J. L.; Vaida, V. *J. Chem. Phys*. **1985**, *83*, 2748.
(4) Donaldson, D. J. *J. Chem. Phys*. **1989**, *91*, 7455.
(5) Beatty, S.; Shiell, R. C.; Chang, D.; Hepburn, J. W. *J. Chem. Phys*. **1999**, *110*, 8476.
(6) Hara, K.; Phillips, D. *Trans. Faraday Soc*. **1978**, *74*, 1441.
(7) Arendt, M. F.; Butler, L. J. *J. Chem. Phys.* **1998**, *109*, 7835.
(8) Roebber, J. L.; Vaida, V. *J. Chem. Phys*. **1985**, *83*, 2748.
(9) Yang, S. C.; Freedman, A.; Kawasaki, M.; Bersohn, R. *J. Chem. Phys*. **1980**, *72*, 4058.
(10) McGivern, W. S.; Sorkhabi, O.; Rizvi, A. H.; Suits, A. G.; North, S. W. *J. Chem. Phys.* **2000**, *112*, 5301.
(11) Addison, M. C.; Donovan, R. J.; Fotakis, C. *Chem. Phys. Lett.* **1980**, *74*, 58.
(12) Black, G.; Jusinski, L. E. *Chem. Phys. Lett*. **1986**, *124*, 90.
(13) Waller, I. M.; Hepburn, J. W. *J. Chem. Phys*. **1987**, *87*, 3261.
(14) Starrs, C.; Jego, M. N.; Mank, A.; Hepburn, J. W. *J. Phys. Chem*. **1992**, *96*, 6526.
(15) Mank, A.; Starrs, C.; Jego, M. N.; Hepburn, J. W. *J. Chem. Phys.* **1996**, *104*, 3609.
(16) McCrary, V. R.; Lu, R.; Zakheim, D.; Russell, J. A.; Halpern, J. B.; Jackson, W. M. *J. Chem. Phys*. **1985**, *83*, 3481.
(17) Liou, H. T.; Dan, P.; Hsu, T. Y.; Yang, H.; Lin, H. M. *Chem. Phys. Lett.* **1992**, *192*, 560.
(18) Li, B.; Myers, A. B. *J. Chem. Phys.* **1991**, *94*, 2458.
(19) Li, B.; Myers, A. B. *J. Chem. Phys*. **1988**, *89*, 6658.
(20) Baronavski, A. P.; Owrutsky, J. C. *Chem. Phys. Lett*. **1994**, *221*, 419.
(21) Farmanara, P.; Stert, V.; Rodloff, W. *J. Chem. Phys*. **1999**, *111*, 5338.
(22) Butler, J. E.; Drozdoski, W. S.; McDonald, J. R. *Chem. Phys*. **1980**, *50*, 413.
(23) Xu, D.; Huang, J.; Jackson, W. M. *J. Chem. Phys*. **2004**, *120*, 3051.
(24) Liou, H. T.; Huang, K. L.; Chen, M. C. *Chem. Phys. Lett.* **1997**, *266*, 591.
(25) Bergeman, T.; Cossart, D. *J. Mol. Spectrosc*. **1981**, *87*, 119.
(26) Kawasaki, M.; Sato, H.; Kobayashi, S.; Arikawa, T. *Chem. Phys. Lett*. **1988**, *146*, 101.
(27) Lee, L. C.; Judge, D. L. *J. Chem. Phys*. **1975**, *63*, 2782.
(28) Frey, J. G.; Felder, P. *Chem. Phys*. **1996**, *202*, 397.